Numerical Simulation of the Collector Angle Effect on the Performance of the Solar Chimney Power Plant

Arkan k. Al-Taaie*   Waheeds S. Mohammad   Abbas J. Jubear***

*, **Department of Mechanical Engineering/ University of Technology*
***Department of Mechanical Engineering /University of Wassit*
***Email: Abbas kut72@yahoo.com.au

Abstract

Sloped solar chimney system is a solar chimney power plant with a sloped collector. Practically, the sloped collector can function as a chimney, then the chimney height can be reduced and the construction cost would be reduced.The continuity, Naver-stockes, energy and radiation transfer equations have been solved and carried out by Fluent software. The governing equations are solved for incompressible, 3-D, steady, turbulent standard $k - \varepsilon$ model with Boussiuesq approximation to develop for the sloped solar chimney system in this study and evaluate the performance of solar chimney power plant in Baghdad city of Iraq numerically by Fluent (14) software with orking conditions such as solar radiation intensity (300,450,600,750 and 900 W/m^2), and collector which angle (0°, 15° and 30°).The results show that the change of collector angle has considerable effects on the performance of the system.The velocity increases when the collector angle increases and reach to the maximize value at a collector angle (30°). The temperature increase with the collector tile angle increase at solar intensity times (7:30,8:15,9,10 AM) but decrease at 12:30 PM) corresponding to solar intensitIes. The study show that Iraqi wather are suitable for this system.

*Keywords***:** *solar chimney; solar energy; collector; natural convection.*

1. Introduction

The solar chimney is a power plant that uses, solar radiation to raise the temperature of the air and, the buoyancy of warm air to accelerate the air stream flowing through the system. The main features of the solar chimney are sketched in Fig.1. Air is heated as a result of the greenhouse effect under a transparent roof (the collector). Because the roof is open around its periphery, the buoyancy of the heated air draws a continuous flow from the roof perimeter into the chimney. A turbine is set in the path of the air current to convert the kinetic energy of the flowing air into electricity.
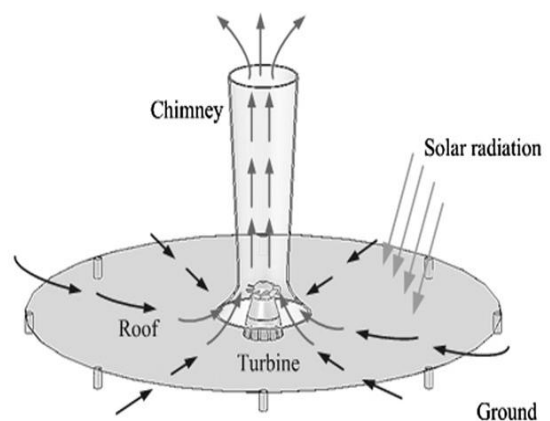

Fig. 1. Schematic layout of the conventional solar chimney power plant. [1]

In 1981 a solar chimney prototype of 50 kW and chimney height nominally at 200 m was built in Manzanares, Spain. The plant operated from 1982 to 1989, and was connected to the local power network between 1986 and 1989 [2]. This project menstruated the viability and reliability of the solar chimney concept Since then, numerous investigations have been conducted to predict the flow in solar chimneys. Generally, it was found that the electricity yielded by a solar chimney is in proportion with the intensity of global solar radiation, collector area and chimney height. Based on a mathematical model, Schlaich [2] reported that optimal dimensions for a solar chimney do not exist. However, if construction costs are taken into account,thermo economically optimal plant configurations may be established for individual sites. Pretorius and Krȯger [3] showed numerically that the power generation is a function of the collector roof shape and inlet height. Ref. [4] Showed analytically that the plant performance depends on the plant size. To overcome the disadvantage of low efficiency, only large-scale plants, in which the chimney heights are 1000 m or more, were proposed in the literature (e.g. [5,6]). As a result, the installation cost of such a plant is very high. Cost analysis for commercial-scaled solar chimney power plants can be found in Refs. [7-10]. To overcome the high investment cost, researchers have proposed some novel and non-conventional concepts. The concept of constructing a solar collector surrounding a hollow space excavated in a mountain was introduced in Ref. [11]. The hollow space can be used as a chimney of the system. It was shown that the cost for constructing a chimney structure can be reduced and the technology would be suitable for mountainous countries. In addition, Papageorgiou proposed the concept of a floating solar chimney technology [12].Ref. [13] proposed a solar chimney system for power production at high latitudes, where sloped lands are readily available and sunshine is at acceptable levels. The authors suggested building a solar chimney collector system on a sloped surface or suitable hill.

A mathematical model and the performance of the solar chimney system with a sloped collector are presented in this paper. This kind of system is hereinafter called the (sloped solar chimney power plant) SSCPP. The analytical models for flows in SSCPP had been proposed in Refs. [13,14,15].While they were useful in their own rights, but the range of application was limited due to the neglect of dynamic pressure

[13] and the exclusion of flow details within the collector ([13,14,15]).

In the present study, a mathematical model that includes the dynamic pressure and the flow details within the collector is developed. As there is no experimental result of SSCPP published,the proposed model is validated by comparing its results with the predictions of the commercial CFD package. Comparisons of the present results with those obtained by other models are also performed.

2. Numurical Implementations

Advanced solver technology provides fast, accurate CFD results, flexible moving and deforming meshes, and superior parallel scalability. Computational Fluid Dynamics (CFD) procedures solve all the interacting governing equations in a coupled manner, albeit in a finite framework. With a careful use of CFD, its results could be used to validate those of the theoretical models, at least qualitatively.

2.1. Modelling in GAMBIT

For the simulation part, the model is designed by using GAMBIT 2.4.6 for those four configurations. This software is provided by the advanced geometry and meshing tools. The functions of GAMBIT are design the three dimensional (3-D) model of three configurations, setup the boundary condition for each edge and faces of each configuration and provide the meshing analysis for each configuration.

The solar chimney power plant was modeled with the following dimensions: Circular absorber ground with a diameter of 6 m , inclined collector angle (θ = 0°,15°and 30°), chimney height 6m,chimney diameter 0.3m and the gap between the absorber and the transparent cover (glass) is 0.1m as shown in Fig.2.
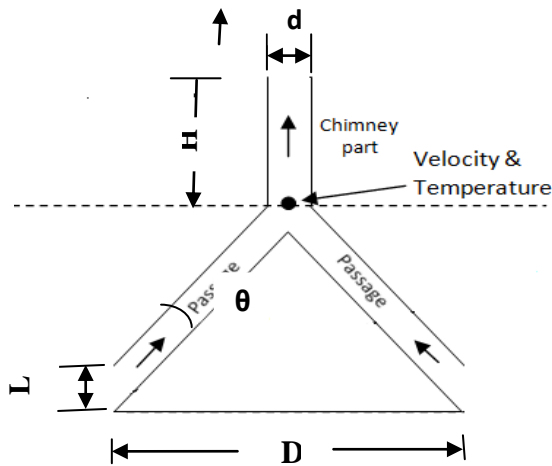
Fig. 2. Physical prototype.

The numerical examination of the flow behavior of air under the steady state condition was studied at both the inlet and the chimney base where the turbine is expected to be staged. The fluid flow calculation was simulated using FLUENT software. The buoyancy driven flow in the system was assumed to be turbulent based on previous studies. Set up the boundary condition is to define the situation occur at the surface condition in term of friction. Meanwhile, defining the meshing is vital in order to discrete each part to certain section for more accuracy FLUENT's analysis. It is important to define, model, meshing, and boundary conditions before running into FLUENT.

Proper boundary conditions are needed for a successful computational work. After it has been to create a geometry where we have one volume where is defined the specify boundary types of solar collector, solar chimney and the base such as the WALL , while the entry and exit zone type is Inlet and Outlet-Pressure. Now The assembly is meshed using tetrahedral elements of T-grid scheme type [16] .Gambit scheme with spacing interval size (0.0275) is chosen as shown in Fig. 3, the Gambit grid generator with approximately 2 million computational cells for different cases. No-slip condition for velocity and temperature on the walls was used.
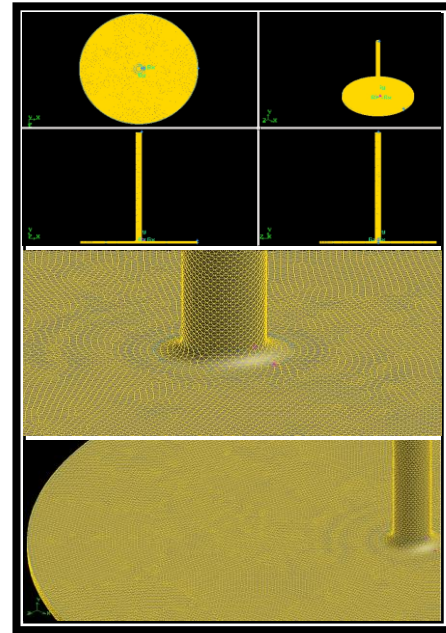

Fig. 3. Computational grid.

2.2. Simulation with FLUENT

FLUENT solves the governing integral equations for the conservation of mass, momentum, energy, and other scalers, such as turbulence.There are two processors used to solve the flow and heat transfer equations. The first preprocessor is the program structure which creates the geometry and grid by using GAMBIT. The second post processor is solving Naver-Stokes equations continuity, momentum and energy.

The set of conservation equations used by CFD are:

Mass conversiotion equation

$$\frac{\partial \rho}{\partial t} + \frac{\partial}{\partial x_i}(\rho \, u_i) = 0 \qquad \ldots \ldots (1)$$

Momentum equation

$$\frac{\partial}{\partial t}(\rho u_i) + \frac{\partial}{\partial x_j}(\rho u_i u_j) = -\frac{\partial p}{\partial x_i} + \frac{\partial}{\partial x_j}$$
$$\left[\mu\left(\frac{\partial u_i}{\partial x_j} + \frac{\partial u_j}{\partial x_i} - \frac{2}{3}\delta_{ij}\frac{\partial u_i}{\partial x_i}\right)\right] +$$
$$\frac{\partial}{\partial x_j}\left(-\rho \overline{u'_i u'_j}\right) \qquad (2)$$

k-ε model equations

$$\frac{\partial}{\partial t}(\rho k) + \frac{\partial}{\partial x_j}(\rho k u_j) =$$
$$\frac{\partial}{\partial x_j}\left[\left(\mu + \frac{\mu_t}{\sigma_k}\right)\frac{\partial k}{\partial x_j}\right] + G_k$$
$$+G_b - \rho\epsilon - Y_M + S_k \qquad (3)$$

81

$$\frac{\partial}{\partial t}(\rho\epsilon) + \frac{\partial}{\partial x_j}(\rho\epsilon u_j) =$$

$$\frac{\partial}{\partial x_j}\left[\left(\mu + \frac{\mu_t}{\sigma_\epsilon}\right)\frac{\partial\epsilon}{\partial x_j}\right] +$$

$$\rho C_1 S_\epsilon - \rho C_2 \frac{\epsilon^2}{k + \sqrt{\nu\epsilon}} + C_{1\epsilon}\frac{\epsilon}{k}C_{3\epsilon}G_b) + S_\epsilon \quad (4)$$

$$C_1 = max\left[0.43, \frac{\eta}{\eta + 5}\right], \eta = S\frac{k}{\epsilon}, S = \sqrt{2S_{ij}S_{ij}}$$

Bousunesq approximation:

$$-\rho\overline{u_i'u_j'} = \mu_t\left(\frac{\partial u_i}{\partial x_j} + \frac{\partial u_j}{\partial x_i}\right) -$$

$$\frac{2}{3}\left(\rho k + \mu_t \frac{\partial u_k}{\partial x_k}\right)\delta_{ij} \quad (5)$$

The viscous medium is also taken.The analysis is carried out using turbulent flow and then the standard k-epsilon and standard wall functions near wall functions [17]. The Discrete Ordinates (DO) was selected under the solar load model enables radiation heat transfer. Define the the Sun Direction Vector, by enter the values for the X, Y, and Z components.

In the current study different direct solar irradiation (300 ,450 ,600 ,750 ,900 W/m^2) data were obtained from Ministry of Transportation-Iraqi Meteorological Organization and Seismology of Baghdad city of 8-8-2008 in the following times (7:30 , 8:15 , 9 ,10 A.M. and 12:30 P.M.) and the sun direction vector is obtained from [18].

Boundary conditions specify the flow and thermal variables on the boundaries of the physical model. They are, therefore, a critical component of the FLUENT simulations and it is important that they are specified appropriately. The boundary conditions applied in this work is shown in Table (1) [19].

Table 1,
Boundary conditions in detail.

Boundary	Type	Boundary condition
Inlet	Pressure-inlet	$\Delta P=0$; T= T$_{ambient}$;
Exit	Pressure-out let	$\Delta P=0$; $T = $ T$_{ambient} - 0.0065*\square chimney\ height$
Ground (asphalt)	Wall	Thermal condition: Mixed h=8 W/m^{2}K;T=T$_{ambint}$
Chimney Wall	Wall	Constant heat flux: q=0
Glass(semi-transparent)	Wall	Thermal condition: Radiation(Thicness=0.004mm

3. Simulation Results

In order to validate the results of the numerical part of the present work, a comparison with the numerical study of [20] was carried out. It can be seen from Figs. (4) and (5) that at the same dimensions of solar chimney power plant a good agreement with the numerical results is achieved of absorbing ground temperature and exit velocity when using asphalt aggregates as an absorption background, at radiation intensities of (310,415,505 W/m^2).
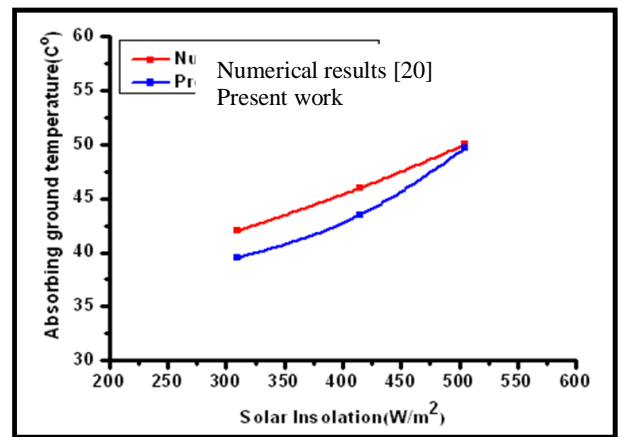

Fig. 4. Comparison of the variation in absorbing ground temperature with solar insolation , with an numerical study [20].
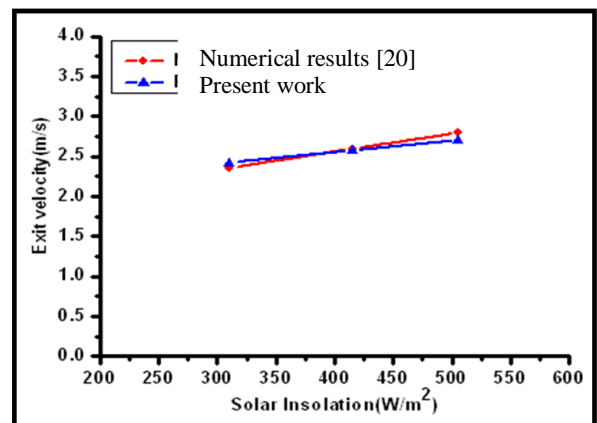

Fig. 5. Comparison of the variation in exit air velocity with solar insolation, with an numerical study[20].

3.1. Variation of the Solar Intensity and Sunlight Direction

The results of the temperature distribution and velocity vectors of solar insolation (300,450,600,750 and 900 W/m^2) at times of

(7:15,8:15,9,10 AM and 12:30 PM) with D=6m ,H= 6m and collector angle (0°, 15°and 30°) regarding the solar chimney passage are presented in Figs. (6 to 23). The increase in air velocity is very small up to about half the radius of the collector. The very steep increase is obtained in the inner half of the collector. This trend is noticed in all solar intensities and sunlight direction as shown in Figs. (7), (10), (13), (16) ,(19) and (22). The reason is due to the combined effect of flow area reduction and the amount of the heat transfer from the ground to the working fluid, which increases the kinetic energy of the flow particles. generally to compare the velocities of the air at the solar collector passage for different solar intensity times (7:30,8:15,9,10 AM and 12:30 PM), it could be seen that the maximum velocity occurs in the (900W/m^2) solar radiation intensity at (12:30 PM) and the minimum velocity in the morning with (300W/m^2) solar intensity at (7:15AM). The numerical solution has shown that the velocity in the center of the chimney is higher than near the wall.

The ground temperature also increases near the collector inlet but show a small decrease near the collector outlet. This is attributed to higher heat transfer coefficients present near the collector counter   as   shown   in Figs.(6),(9),(12),(15),(18),and(21).

The development of flow in the chimney can be seen through the enlargement regions shown in Figs. (8), (11), (14), (17) ,(20),and (23). The flow in the chimney is similar to close conduits viscous forces cause a flow velocity profile to form such that the fluid flows slower close to the walls and a change in the flow type cases a change in the velocity profiled.The flow in the lower and middle regions is developing non uniform flow, but in the top region is uniform fully developed flow (turbulent flow).

The heat transfer model is used to compare the performance of a conventional solar chimney power plant with three collector orientations at (0° , 15°and 30°). Results indicate that the larger collector angle leads to improve performance of the solar chimney in the morning and give rise to the strong influence of the sunlight direction of the velocity and temperature fields.

3.2. Maximum Temperature Difference

The buoyancy driving force takes effect due to the gravity force, so the larger the collector tilt, the stronger the influence of buoyancy effect will be. Fig. (24) presents the temperature difference

for collectors of different tilt angles. The temperature difference increases at the tilt angle increase when the solar intensity is (300,450,600, and 750 W/m^2) but it decreases at (900W/m^2) due to the sunlight direction as it is approximately perpendicular. The slope angle is the angle between the collector and horizontal axis. The absorber used in the collector can get the most efficient energy when it is mounted as the collector axis which is exactly perpendicular to the sun rays. The angle of sun rays changes related to hour and seasonal time, so do the angles and the slops.

3.3. Maximum Velocity

It can be observed from the results shown in Fig. (25) that the solar intensity increased as a result of time. The maximum velocity of the chimney increased too, as collector angle increases due to changes in the incident angle of the solar radiation and the maximum velocity occur when the collector angle was 30°.
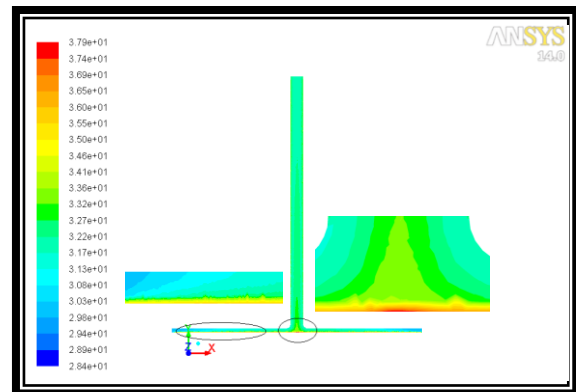

Fig. 6. Contours of temperature distribution for solar chimney with solar insolation (300 W/m^2) for D=6m, H=6m, θ=0°.

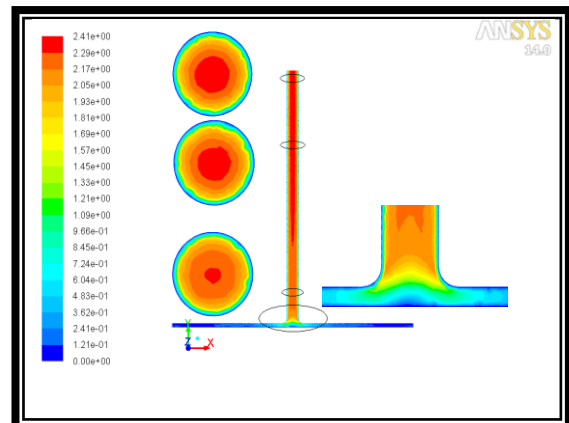**Fig. 7. Contours of velocity distribution for the solar chimney with solar insolation (300 W/m^2) for D=6m, H=6m θ=0°.**
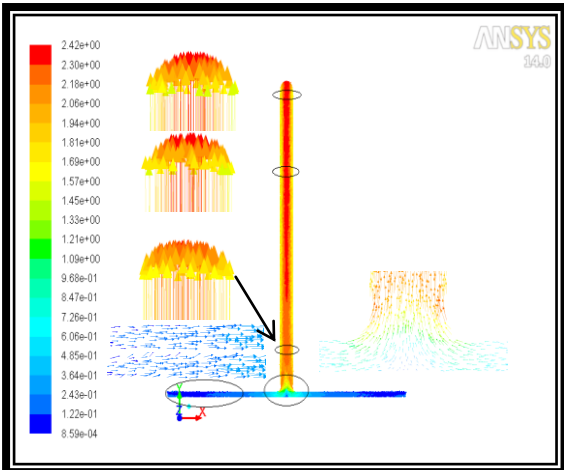
Fig. 8. Flow felid of air in solar chimney with solar insolation (300 W/m²) for D=6m, H=6m, θ=0°.
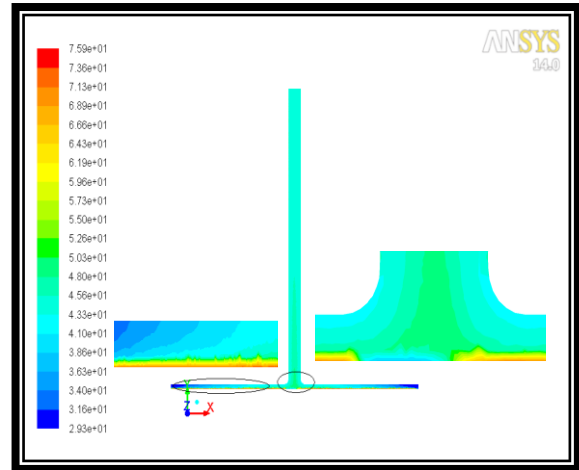
Fig. 9. Contours of temperature distribution for solar chimney with solar insolation (900 W/m²) for D=6m, H=6m, θ=0°.
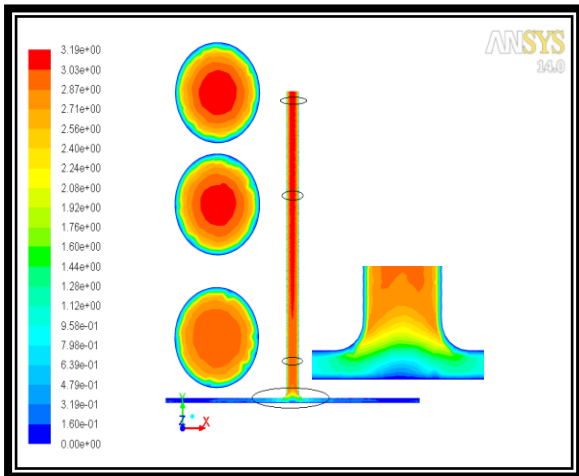
Fig. 10. Contours of velocity distribution for solar chimney with solar insolation (900 W/m²) for D=6m, H=6m, θ=0°.
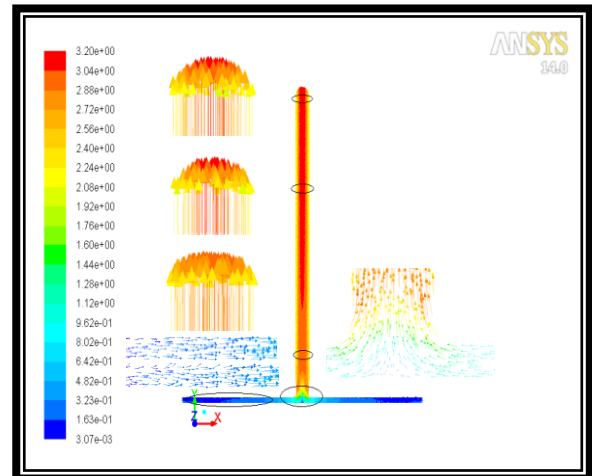
Fig. 11. Flow felid of air in solar chimney with solar insolation (900 W/m²) for D=6m, H=6m, θ=0°.
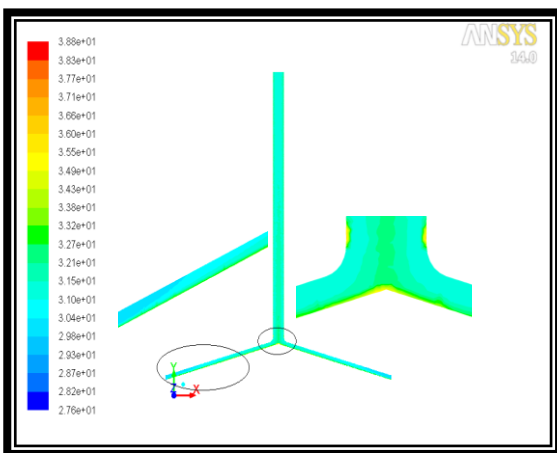
Fig. 12. Contours of temperature distribution for solar chimney with solar insolation (300 W/m²) for D=6m, H=6m, θ =15°.
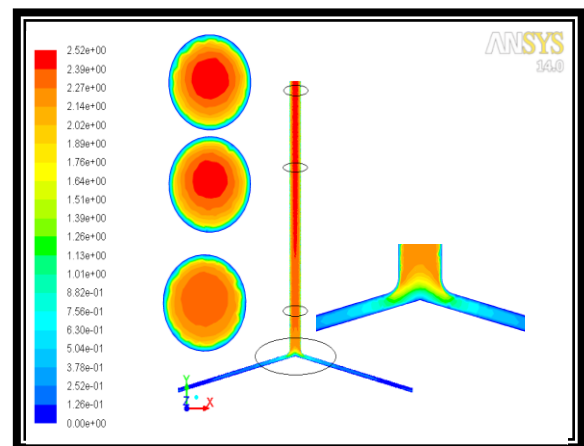
Fig .13. Contours of velocity distribution for solar chimney with solar insolation (300 W/m²) for D=6m, H=6m, θ=15°.

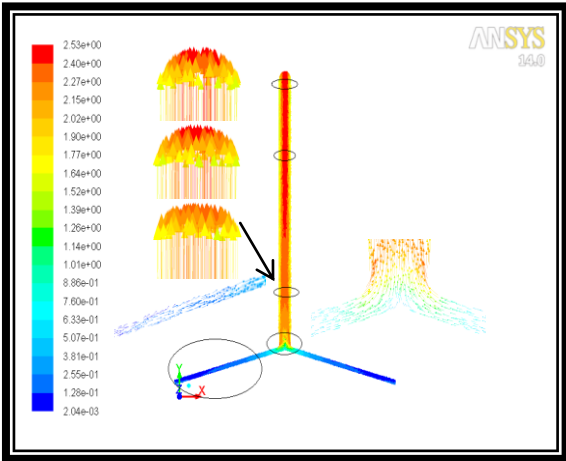**Fig. 14. Flow felid of air in solar chimney with solar insolation (300 W/m^2) for D=6m, H=6m, θ=15.**
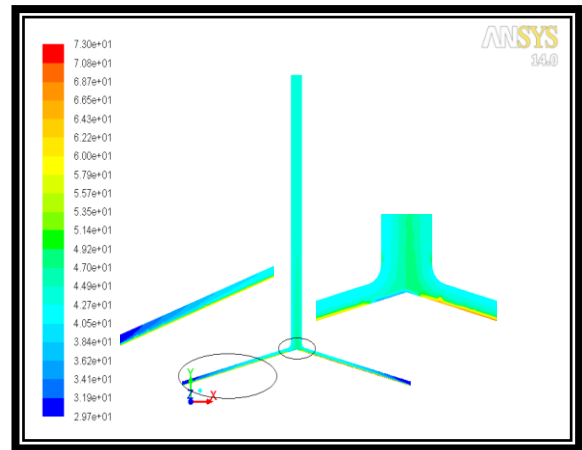
Fig. 15. Contours of temperature distribution for solar chimney with solar insolation (900 W/m^2) for D=6m, H=6m, θ =15°.
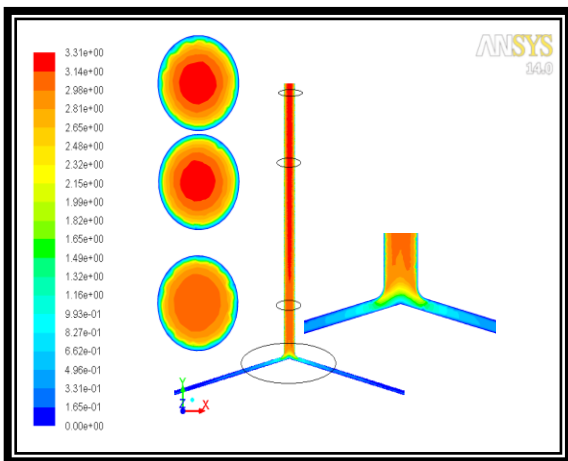

Fig. 16. Contours of velocity distribution for solar chimney with solar insolation (900 W/m^2) for D=6m, H=6m, θ =15°.

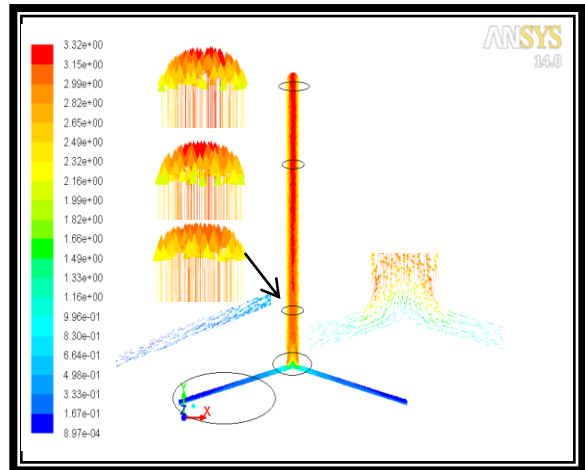**Fig. 17. Flow felid of air in solar chimney with solar insolation (900 W/m^2) for D=6m, H=6m, θ =15°.**

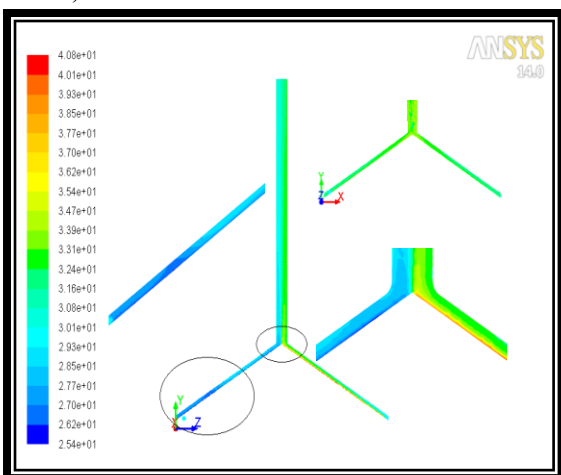**Fig. 18. Contours of temperature distribution for solar chimney with solar insolation (300 W/m^2) for D=6m, H=6m, θ =30°.**
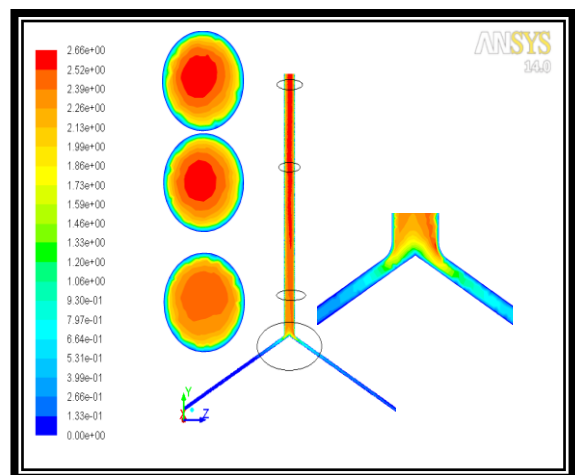
Fig .19. Contours of velocity distribution for solar chimney with solar insolation (300 W/m^2) for D=6m, H=6m, θ =30°.
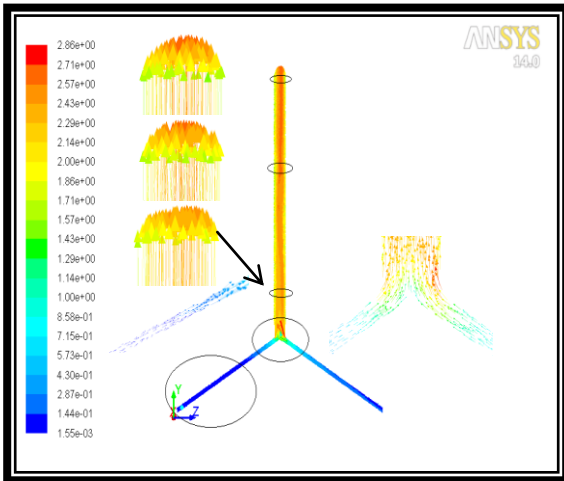
Fig. 20. Flow felid of air in solar chimney with solar insolation (300 W/m^2) for D=6m, H=6m, θ

Fig. 21.Contours of temperature distribution for solar chimney with solar insolation (900 W/m^2) for D=6m, H=6m, θ =30°.
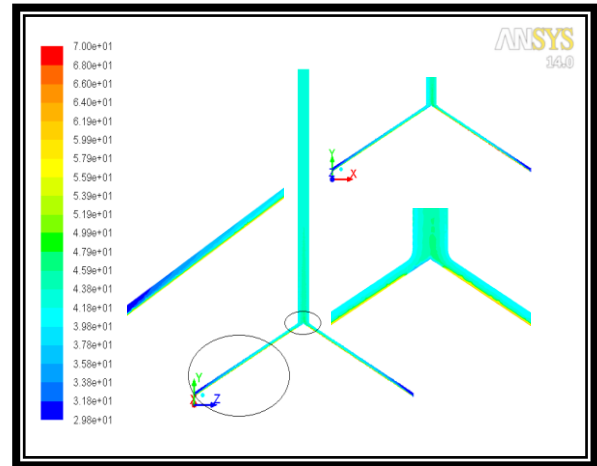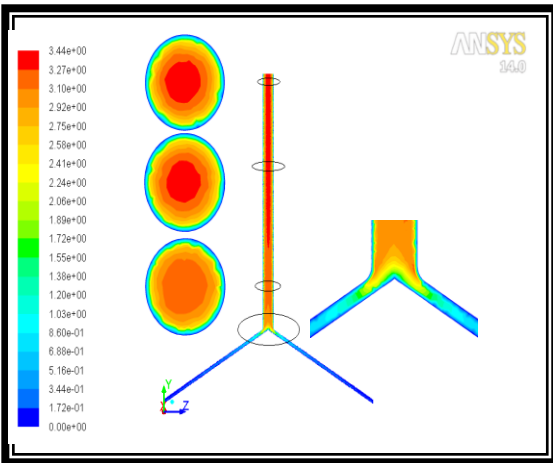

Fig. 22. Contours of velocity distribution for solar chimney with solar insolation (900 W/m^2) for D=6m, H=6m, θ =30°.
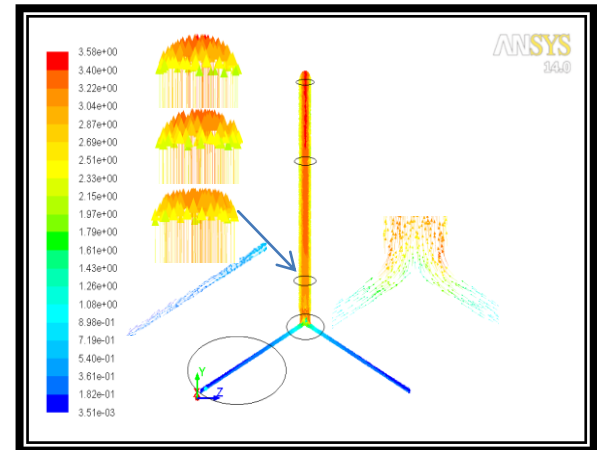
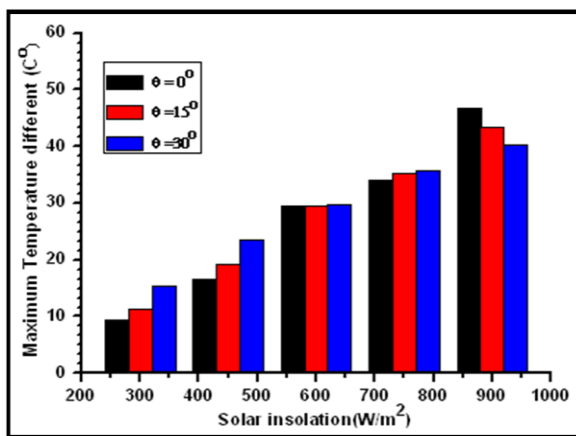**Fig. 23. Flow felid of air in solar chimney with solar insolation (900 W/m^2) for D=6m, H=6m, θ= 30°.**

Fig. 24. The effect of collector angle on maximum temperature at difference solar insolation for D =6m.
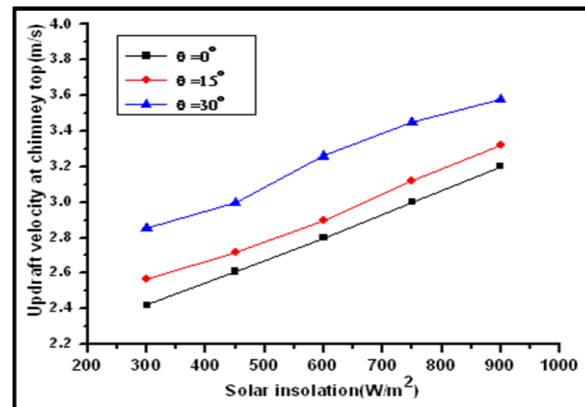

Fig. 25. The effect of collector angle on updraft velocity at chimney top at different solar insolation for D =6m.

86

4. Conclution

A numerical model for the sloped solar chimney power plant is proposed. The model includes a flow detail inside a collector and chimney. Numerical simulations were conducted in order to evaluate the performance of sloped solar chimney power plants. The relationships between the collector angle, the temperature rise across the collector and velocity at chimney are presented. This observation would be useful in the preliminary plant design. The results show:

1. The numerical results of this study have a good agreement with the numerical results of [20] at the same conditions and ($\theta=0°$).
2. The temperature increases with the collector tile angle increase at solar intensity times (7:30,8:15,9 and 10 AM) but decrease at 12:30 PM).
3. The velocity of air increase as collector angle increase and maximum velocity occurs at collector angle 30°.
4. Both, maximum air temperature and exit air velocity were at solar radiation intensity; 900 W/m2.
5. the cost for constructing a chimney structure can be reduced as a result of reduction in the chimney height.
6. Under the Iraq weather radiation conditions, large scale solar chimney in Iraq is recommended and use the hills and mountains that are available to build these plants.

Symbols and Acronyms

Symbol	Description	Unit
D	Diameter of absorbing ground	m
g	Gravitational acceleration	m/s^2
H	Chimney height	m
h	Heat transfer coefficient	W/m^{2}k
I	Solar radiation	W/m^2
K	Turbulent kinetic energy	m^2/s^2
L	Periphery height of the collector: 0.1	m
p	Pressure	Pa
r	Radius	m
S$_\phi$	General source term	
T	Temperature	K°
T$_{Max}$	Maximum Temperature	K°
t	Time	s
u', v'	Fluctuation of mean velocities	m/s
U,V,W	Time-average velocity	m/s
u, v,w	Velocity components (x,y&z) direction	m/s
Δ	Differentive	
α	Absorbtance	
∂	Partial derivative	
ε	Rate of dissipation of kinetic energy	m^2/s^2
θ	Angle	degree
ρ	Fluid density	kg/m^3
ϕ	General dependent variable	
μ	Dynamic viscosity	N.s/m^2
μ$_t$	Turbulent viscosity	N.s/m^2
π	Pi	
o	Ambient	

5. References

[1] Atit, K.and Tawit, C.," Accuracy of theoretical models in the prediction of solar chimney performance", Solar Energy. Vol. 83, PP. (1764-1771), 2009.
[2] Schlaich J., "The solar chimney", Edition Axel Menges, Stuttgart, Germany, 1995.
[3] Pretorius J.P., Kroger D.G., "Solar chimney power plant performance", J. Sol. Energy Eng. Vol.128, 2006,pp 302–311.
[4] Lorente S, Koonsrisuk A, Bejan A. "Constructal distribution of solar chimney power plants few large and many small". International Journal of Green Energy 2010;7(6):pp. 577-592.
[5] Rohmann M. "Solar chimney power plant". Bochum University of Applied Sciences; 2000.
[6] "EnviroMission's solar tower of power", http://seekingalpha.com/article/14935-enviromission-s-solar-tower-of-power; 2006.
[7] Schlaich J. "The solar chimney " Stuttgart, Germany: Edition Axel Menges; 1995.
[8] Schlaich J, Bergermann R, Schiel W, "Weinrebe G. Sustainable electricity generation with solar updraft towers". Structural Engineering International 2004;14(3):,pp. 225-229.
[9] Fluri TP, Pretorius JP, Van Dyk C, Von Backström TW, Kröger DG, Van Zijl GPAG.

"Cost analysis of solar chimney power plants. Solar Energy" 2009;83(2):,pp. 246-256.

[10] Nizetic S, Ninic N, Klarin B. "Analysis and feasibility of implementing solar chimney power plants in the Mediterranean region. Energy 2008;33(11):,pp.1680-1690.

[11] Zhou XP, Yang JK, Wang J, Xiao B. "Novel concept for producing energy integrating a solar collector with a man made mountain hollow". Energy Conversion and Management 2009;50(3):pp. 847-854.

[12] Papageorgiou C. "Floating solar chimney technology". In: Rugescu RD, editor.Solar energy. INTECH; 2010.

[13] Bilgen E, Rheault J. "Solar chimney power plants for high latitudes". Solar Energy 2005;79(5):,pp. 449-458.

[14] Cao F, Zhao L, Guo L." Simulation of a sloped solar chimney power plant in Lanzhou". Energy Conversion and Management 2011;52(6):,pp. 2360-2366.

[15] Panse SV, Jadhav AS, Gudekar AS, Joshi JB. "Inclined solar chimney for power production". Energy Conversion and Management 2011;52(10):,pp. 3096-3102.

[16] Jianhua F., Louise J.and Simon F.," Flow distribution in a solar collector panel with horizontally inclined absorber strips", http://www.sciencedirect.com, Solar Energy, Vol. 81, PP. (1501–1511),2007.

[17] Launder, B. E. and Spalding, D. B., "Lectures in mathematical models of turbulence", Academic Press, London, England, 1972.

[18] John A. Duffie,"Solar engineering of thermal processes" , Book, John Wiley and SONS , INC.,Second Edition, 1980.

[19] Ming T., Liu W., and Xu G.." Analytical and numerical investigation of the solar chimney power plant systems", International Journal of Energy Research, Vol. 30, Issue 11, PP. (861–873), September 2006.

[20] Rafah A. N.,"Numerical Prediction of a solar chimney performance using CFD technique" ,Ph.D. Thesis Submitted to Electromechanical Engineering Department University of Technology Baghdad, 2007.

نمذجة رقمية لتاثير زاوية المجمع على سلوك الجريان في منظومة مدخنة شمسية لتوليد القدرة

اركان خلخال حسين*   وحيد شاتي محمد**   عباس جاسم جبير***

*،** قسم الهندسة الميكانيكية/ الجامعة التكنولوجية

***قسم الهندسة الميكانيكية/ جامعة واسط

البريد الالكتروني: Abbaskut72@yahoo.com.au*

الخلاصة

ان نظام المدخنة الشمسية المائل عبارة عن مدخنة قدرة شمسية يكون فيها وضع المجمع الشم سي مائلا بزاوية والذي يمكن وصفه دالة للمدخنة،حيث بالامكان تخفيض كلفة انشاء المدخنة وذلك بسبب التخفيض الذي سوف يحصل في ارتفاع ال مدخنة.تم حل معادلات الاستمرارية والزخم و الطاقة والاشعاع الشمسي باستخدام برنامج(14) Fluent.في هذه الدراسة تم اختبار اداء المدخنة الشمسية المائلة خلال جريان لانضغاطي ،ثلاثي الابعاد، مستقر واضطرابي حيث تم الاستعانة بالموديل الاضطرابي k-ε وذاك لحساب اداء المدخنة الشمسية تحليليا في اجواء بغداد- العراق،حيث كانت ابعاد المدخنة الشمسية الارتفاع 6 م ،قطر المجمع 6م،قطر المدخنة 0.3 م وارتفاع مدخل المجمع 0.1 م وذلك عند ظروف اختبار مختلفة ،شدة الاشعاع الشمسي(300 و 450 و 600 و 750 و900) واط/م² وعند زويا ميل مختلفة للمجمع (0°, 15°, 30°) من ابرز النتائج ا لتي توصل لها البحث هو التاثير الكبير لتغير زاوية المجمع الشمسي على اداء المدخنة الشمسية.حيث نلاحظ ازدياد سرعة الهواء داخل المدخنة بزيادة زاوية ميلان المجمع حث تصل الى اقصى قيمه عند زاوية 30° ،تم التوصل كذلك ان درجات الحرارة تزداد بزيادة زاوية المجمع الشمسي في الاوقات (10,9,15:8,7:30 ق ظ) والمناظرة لشدة الاشعاع الشمسي وتقل عند (12:30) ب ظ. بينت هذه الدراسة ايضا ان اجواء العراق ملائمة لهذا النوع من الانظمة.